EARTHQUAKE ENGINEERING AND STRUCTURAL DYNAMICS
Earthquake Engng. Struct. Dyn. **27**, 1203–1224 (1998)

LIMITS OF ACHIEVABLE PERFORMANCE AND CONTROLLER DESIGN FOR THE STRUCTURAL CONTROL BENCHMARK PROBLEM

FERNANDO J. D'AMATO AND MARIO A. ROTEA*
School of Aeronautics and Astronautics, Purdue University, West Lafayette, IN 47907-1282, U.S.A.

SUMMARY

In this work we give a methodology for controller design and analysis which accounts for design criteria such as: (a) optimal system response to external disturbances, (b) robustness to modelling uncertainty, and (c) constraints on the controller order. The methodology is applied to a structural control benchmark problem sponsored by the ASCE Committee on Structural Control. The structural system considered consists of a scale model of a three-storey building employing an active mass driver to suppress ground motion disturbances. The methodology proved effective for obtaining a satisfactory low-order controller for this class of problems. © 1998 John Wiley & Sons, Ltd.

KEY WORDS: active control of structures; multi-objective optimization; robust control; optimal response to seismic loads

1. INTRODUCTION

The goal of this paper is to report on a methodology for controller design and analysis which accounts for design criteria such as (a) optimal system response to external disturbances, (b) robustness to modelling uncertainty, and (c) constraints on the controller order. The methodology does not include all of these objectives in the design stage; instead, a subset of objectives is optimized to produce a *family* of controllers that is screened later using the remaining criteria. The outcome of this screening process is the final controller.

We have used this methodology to design controllers for the structural control benchmark problems.[1] To keep this paper to a manageable size, we present the result for the first benchmark problem only. Briefly, the solution we obtained for this problem has the following features:

(1) Eighth-order stable controller.
(2) The structural responses (interstory drifts and floor accelerations), to random ground disturbances, are reduced by 63 per cent; these responses are optimal.
(3) The structural responses, to the Hachinohe and El Centro earthquakes, are reduced by 39 per cent.
(4) The hard constraints on commanded actuator voltage, displacement and acceleration of the active mass driver, are all met.

* Correspondence to: Mario A. Rotea, School of Aeronautics and Astronautics, Purdue University, West Lafayette, IN 47907-1282, U.S.A. E-mail: rotea@ecn.purdue.edu

Contract/grant sponsor: National Science Foundation; Contract/grant number: ECS-9358288
Contract/grant sponsor: Boeing
Contract/grant sponsor: United Technologies Corporations

CCC 0098–8847/98/111203–22$17·50

Received 15 May 1997
Revised 12 December 1997

(5) The compensated loop gain is less than -20 db at all frequencies outside the range 5–31 Hz; thus, the control bandwidth contains the first three structural modes only, and it ensures robustness of stability and performance to unmodelled dynamics.
(6) robust stability is guaranteed for simultaneous variations in the first three structural modes (the controlled modes) of at least 21 per cent in natural frequencies and 53 per cent in damping ratios.

The paper contains five more sections and three appendices. In Section 2, we give a brief description of the design model. Section 3 summarizes the evaluation criteria, and controller implementation constraints, of the benchmark problem. The methodology for controller design and analysis is in Section 4. A key contribution of this section, which should prove useful to other groups working in the benchmark problem, is the optimal tradeoff surface between the system response to random disturbances and the cost of actuation. This surface can be used to make quantititative comparisons among the controllers obtained for the first benchmark problem. Controller order reduction and robustness analysis tests are part of the methodology and they are included in Section 4 also. Section 5 contains the results of the time-domain simulations performed with the SIMULINK model introduced in Reference 1. The appendices summarize the methods and tools required to implement our methodology.

2. DESIGN MODEL

The model used for controller design and analysis is the evaluation model described in Reference 1. This model has 28 states and it is given by the following equations:

$$\dot{x} = Ax + E\ddot{x}_g + Bu \tag{1a}$$

$$y = C_y x + F_y \ddot{x}_g + D_y u \tag{1b}$$

where x is the state vector, $\ddot{x}_g$ is the ground acceleration, u is a scalar control input, and y is the measurement vector available to the controller. The measurement vector y is partitioned into $y^T = [\, y_1^T y_2]$, where

$$y_1 = \begin{bmatrix} x_m \\ \ddot{x}_{a1} \\ \ddot{x}_{a2} \\ \ddot{x}_{a3} \\ \ddot{x}_{am} \end{bmatrix} \quad \text{and} \quad y_2 = \ddot{x}_g \tag{2}$$

The units of the control input u and the measurement y are volts; thus, the input–output map from u to y is non-dimensional.

No attempt is made to reduce the order of the model for design purposes. This is because the number of states is within the range that can be handled by the design methods used in this paper.

The controllers are designed using continuous-time methods without taking into account time/amplitude quantizations; these discretizations are incorporated later to obtain the implementable control laws. The notation used for the ideal control law is

$$u = C_1 y_1 + C_2 y_2 \tag{3}$$

where C_1 and C_2 denote continuous-time linear time-invariant dynamical systems; C_1 is a *feedback* controller while C_2 is a *feedforward* controller. The notation used for the overall controller is

$$C = [C_1 \; C_2] \tag{4}$$

3. EVALUATION CRITERIA AND IMPLEMENTATION CONSTRAINTS

The evaluation criteria and implementation constraints are defined in Reference 1 and repeated here for completeness.

3.1. Stochastic evaluation criteria

In this case, the ground acceleration $\ddot{x}_g$ is a stationary stochastic process with power spectral density

$$S_{\ddot{x}_g\ddot{x}_g}(\omega, \omega_g, \zeta_g) = S_0(\omega_g, \zeta_g)\frac{4\zeta_g^2\omega_g^2\omega^2 + \omega^4}{(\omega^2 - \omega_g^2)^2 + 4\zeta_g^2\omega_g^2\omega^2} \tag{5}$$

where the natural frequency ω_g and the damping ratio ζ_g lie in prescribed intervals. The scaling factor S_0 keeps constant the rms value of the ground acceleration irrespective of changes in ω_g and ζ_g.

In addition to this ground disturbance, the entire measurement vector y is corrupted by the measurement noise v. Each component of the measurement noise is modelled as a stationary white noise process.

When both the random ground disturbance and the measurement noise are applied to the sructure, the effectiveness of the controller is to be measured by the following criteria:†

$$J_1 = \max\left\{\frac{\sigma_{d1}}{\sigma_{x_{30}}}, \frac{\sigma_{d2}}{\sigma_{x_{30}}}, \frac{\sigma_{d3}}{\sigma_{x_{30}}}\right\} \tag{6a}$$

$$J_2 = \max\left\{\frac{\sigma_{\ddot{x}_{a1}}}{\sigma_{\ddot{x}_{a30}}}, \frac{\sigma_{\ddot{x}_{a2}}}{\sigma_{\ddot{x}_{a30}}}, \frac{\sigma_{\ddot{x}_{a3}}}{\sigma_{\ddot{x}_{a30}}}\right\} \tag{6b}$$

$$J_3 = \max\left\{\frac{\sigma_{x_m}}{\sigma_{x_{30}}}\right\} \tag{6c}$$

$$J_4 = \left\{\frac{\sigma_{\dot{x}_m}}{\sigma_{\dot{x}_{30}}}\right\} \tag{6d}$$

$$J_5 = \max\left\{\frac{\sigma_{\ddot{x}_{am}}}{\sigma_{\ddot{x}_{a30}}}\right\} \tag{6e}$$

where the inter-storey drifts d_i are the relative lateral displacements between floors ($d_1 = x_1$, $d_2 = x_2 - x_1$, $d_3 = x_3 - x_2$), $\dot{x}_i$ is the lateral velocity of floor i, and $\ddot{x}_{ai}$ represents the absolute lateral acceleration of floor i. The signals x_m, $\dot{x}_m$ and $\ddot{x}_{am}$ are the displacement (relative to the 3rd floor), velocity and absolute acceleration of the active mass driver. Finally, the normalization constants $\sigma_{x_{30}}$, $\sigma_{\dot{x}_{30}}$, and $\sigma_{\ddot{x}_{a30}}$ are, respectively, the worst-case rms values of the 3rd floor position, velocity and absolute acceleration, over all allowed values of ω_g and ζ_g, when the loop is open.

In addition, the following hard constraints must be met:

$$\sigma_u \leqslant 1 \text{ V}, \quad \sigma_{\ddot{x}_{am}} \leqslant 2g, \quad \sigma_{x_m} \leqslant 3 \text{ cm} \tag{7}$$

Criteria (6) and the rms values defining the constraints (7) depend on the parameters ω_g and ζ_g of the disturbance model (5). When evaluating the criteria, and constraints, for a given controller, these quantities need to be maximized over ω_g and ζ_g to determine the worst possible values. This is to be done using the following ranges:

$$3{\cdot}18 \text{ Hz} \leqslant \omega_g \leqslant 19{\cdot}1 \text{ Hz}, \; 0{\cdot}3 \leqslant \zeta_g \leqslant 0{\cdot}7 \tag{8}$$

† We use the symbol σ_x to denote the rms value of a stochastic signal x

3.2. Deterministic evaluation criteria

In this case, the ground acceleration is one of two historical earthquake records: 1940 El Centro NS and 1968 Hachinohe NS. The controller is evaluated according to the following criteria:

$$J_6 = \max_{\substack{\text{El Centre}\\ \text{Hachinohe}}} \max_t \left\{ \frac{|d_1(t)|}{x_{30}}, \frac{|d_2(t)|}{x_{30}}, \frac{|d_3(t)|}{x_{30}} \right\} \tag{9a}$$

$$J_7 = \max_{\substack{\text{El Centro}\\ \text{Hachinohe}}} \max_t \left\{ \frac{|\ddot{x}_{a1}(t)|}{\ddot{x}_{a30}}, \frac{|\ddot{x}_{a2}(t)|}{\ddot{x}_{a30}}, \frac{|\ddot{x}_{a3}(t)|}{\ddot{x}_{a30}} \right\} \tag{9b}$$

$$J_8 = \max_{\substack{\text{El Centro}\\ \text{Hachinohe}}} \max_t \frac{|x_m(t)|}{x_{30}} \tag{9c}$$

$$J_9 = \max_{\substack{\text{El Centro}\\ \text{Hachinohe}}} \max_t \frac{|\dot{x}_m(t)|}{\dot{x}_{30}} \tag{9d}$$

$$J_{10} = \max_{\substack{\text{El Centro}\\ \text{Hachinohe}}} \max_t \frac{|\ddot{x}_{am}(t)|}{\ddot{x}_{a30}} \tag{9e}$$

where x_{30}, $\dot{x}_{30}$ and $\ddot{x}_{a30}$ are the largest peak values, taken over both earthquake records, of the 3rd floor position, velocity and absolute acceleration, respectively, when no controller is present.

In addition, the following hard constraints must be met

$$\max_{\substack{\text{El Centro}\\ \text{Hachinohe}}} \max_t |u(t)| \leqslant 3 \text{ V} \tag{10a}$$

$$\max_{\substack{\text{El Centro}\\ \text{Hachinohe}}} \max_t |\ddot{x}_{am}(t)| \leqslant 6g \tag{10b}$$

$$\max_{\substack{\text{El Centro}\\ \text{Hachinohe}}} \max_t |x_m(t)| \leqslant 9 \text{ cm}. \tag{10c}$$

3.3. Implementation constraints

The controller for the structural control benchmark problem must be delivered in discrete time.[1] The discrete-time controller is to operate at 1 kHz sampling rate, and it must satisfy the following implementation constraints: (a) open-loop stable, and (b) order no higher than 12 states.

4. OPTIMIZATION-BASED DESIGN METHODOLOGY

In this section we formulate the controller design problem as a multiobjective optimization problem. The precise steps used for controller design are shown below.

1. Select the *nominal* parameters ω_g and ζ_g for the random ground disturbance model in equation (5), within the ranges shown in equation (8), which will be used for controller design.
2. Using the disturbance model selected in step 1, compute the *optimal tradeoff surface* between the stochastic actuation costs and stochastic structural response, subject to the hard constraints (7). This step produces a *set* of controllers that optimizes the stochastic structural response and the stochastic actuation costs.

3. Reduce the order of the optimal controllers obtained in step 2 to generate a set of low-order controllers that meet the stochastic hard constraints, and whose structural responses and actuation costs are as close as possible to the optimal tradeoff surface computed in step 2.
4. Compute the subset of low-order controllers that meet the deterministic hard constraints (10).
5. Analyse the robustness to variations in the disturbance model (5), variations in structural parameters, and unmodelled dynamics, of the set of low order controllers computed in step 4 and select a final candidate for implementation.

4.1. Achievable performance with stochastic disturbances

Given the parameters, ω_g and ζ_g, of the disturbance model (5), and a controller, the structural response of the system can be measured by the single performance measure

$$J_{per} = \max\{r_1 J_1, J_2\} \tag{11}$$

where the positive number r_1 provides the relative weight between the interstorey drifts (J_1) and floor absolute accelerations (J_2). The actuation cost can be measured by

$$J_{act} = \max\{r_3 J_3, r_4 J_4, J_5\} \tag{12}$$

where r_3 and r_4 are positive numbers providing relative weighting among the actuator displacement (J_3), actuator velocity (J_4) and actuator acceleration (J_5).

Performance improvement, i.e. reduction of J_{per}, can only be obtained at the expense of an increase in J_{act}. The optimal tradeoff between J_{per} and J_{act} may be computed by solving the following constrained optimization problem:

$$\begin{aligned} J_{act}^{OPT}(q) = \min \quad & J_{act} \\ \text{subject to} \quad & J_{per} \leqslant q J_{per}^{OL} \\ & \sigma_u \leqslant 1 \text{ V}, \sigma_{x_{am}} \leqslant 3 \text{ cm}, \sigma_{\ddot{x}_{am}} \leqslant 2g \end{aligned} \tag{13}$$

where J_{per}^{OL} is the performance cost for the open-loop system, the parameter q satisfies the inequality $0 \leqslant q \leqslant 1$, and the minimization is performed over all the controllers C (see equation (4)) that stabilize the system.

A solution to problem (13) gives a controller that satisfies the stochastic hard constraints (7), and achieves a performance cost J_{per} no greater than $q\, J_{per}^{OL}$ with the least possible actuation effort. By sweeping q between zero and one, the tradeoff curve between J_{per} and J_{act} may be generated. This gives a family of controllers which are Pareto optimal for the costs J_{per} and J_{act} when the hard constraints are met. This family may be screened for other performance measures and/or robustness properties to select the final controller candidates. Details for solving equation (13) are given in Appendix I.

The parameters used for solving problem (13) are shown in Table I. The relative weights r_1, r_3 and r_4 are taken to be one because no information justifying the preference of one cost over another was provided. We take the nominal values of ω_g and ζ_g to be the worst-case for the uncontrolled (open-loop) structure. In this problem this is a very logical choice. Partly, this is because to improve the structural response,

Table I. Parameters for problem (13)

ω_g	ζ_g	r_1	r_3	r_4
5·94 Hz	0·3	1	1	1

with the least actuation effort, the controller should increase the damping of the modes that define performance without changing their natural frequencies. Later, it will be shown that our designs do satisfy this property.

Figure 1 gives the tradeoff curve between J_{per} and J_{act}. This figure is obtained by solving problem (13), with $0{\cdot}19 \leqslant q \leqslant 0{\cdot}63$, and plotting $J_{per}(q)$ against its corresponding value of $J_{act}^{OPT}(q)$. This result states that there exists no stabilizing controller meeting the stochastic hard constraints with both J_{act} and J_{per} below the optimal tradeoff curve. The individual costs J_1 to J_5 and the rms values of u, x_m and $\ddot{x}_{am}$ are plotted against q in Figure 2. Frames (3, 2), (4, 1) and (4, 2), show that the hard constraints (7) and (10) are met.

The tradeoff curve in Figure 1 should prove useful to other groups working with the benchmark problem for this curve can be used to make quantitative comparisons among the controllers obtained for the first benchmark problem.

4.2. *Controller reduction*

The controllers lying on the optimal tradeoff plot of Figure 1 have order 30. These controllers were reduced applying the weighted balance and truncation method on a coprime factorization of the controllers. The weight was selected to guarantee closed-loop stability with the reduced-order controllers. As left and right coprime factor reduction can give different results, both methods were applied. Details of the methods are given in Appendix II. Using this method a set of tenth-order controllers was obtained.

The tradeoff, between J_{act} and J_{per}, achieved by the reduced-order controllers is shown Figure 3. This set of tenth-order controllers is practically optimal. The individual costs J_1 to J_5, and rms values of the signals that must satisy hard constraints, are plotted in Figure 4 together with the optimal ones. There is no difference between the optimal values and the values attained by the reduced-order controllers.

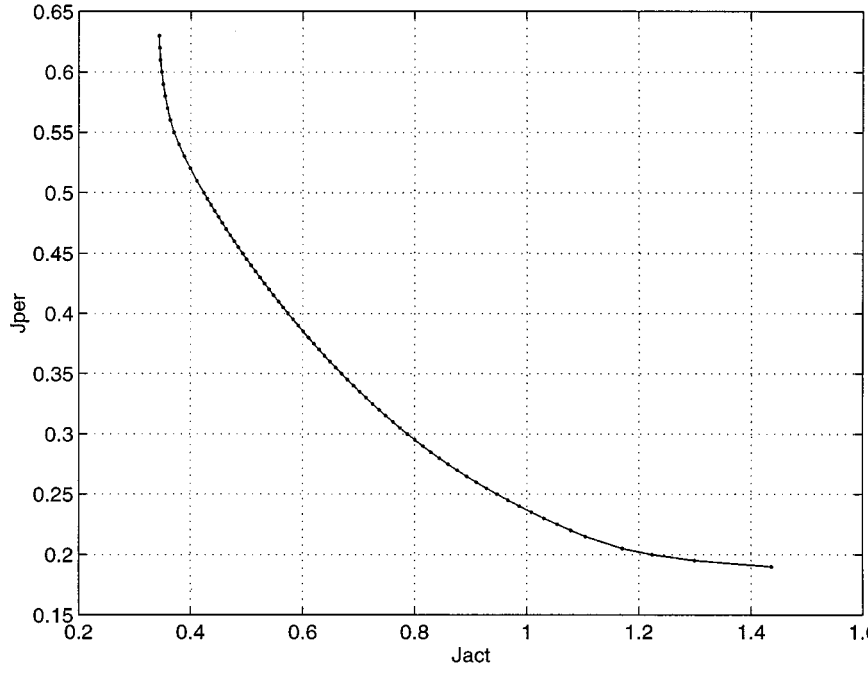

Figure 1. Optimal tradeoff between performance and actuation costs—random disturbances

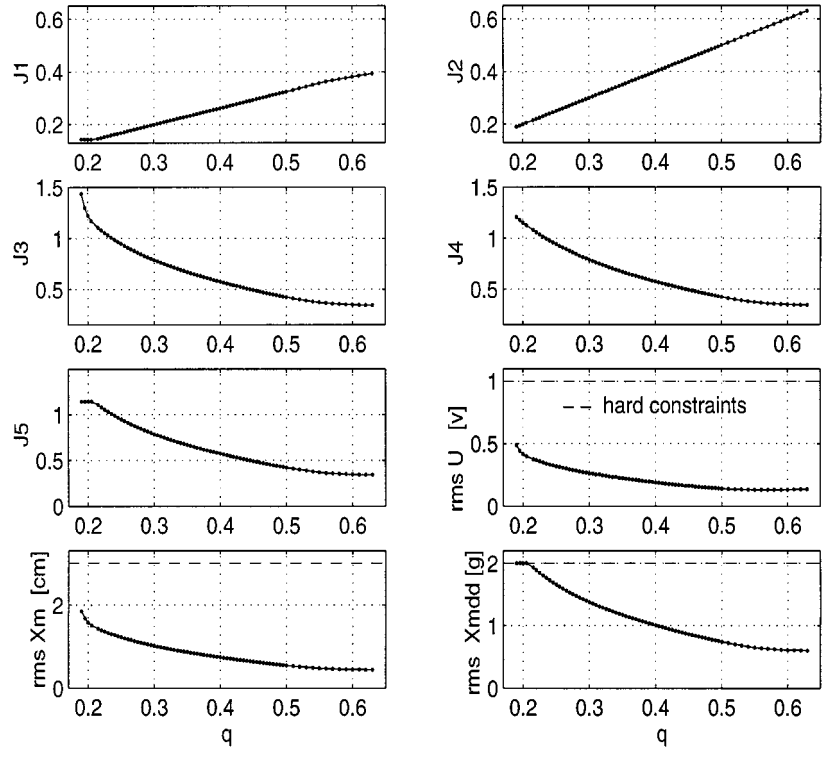

Figure 2. Optimal evaluation criteria—random disturbances

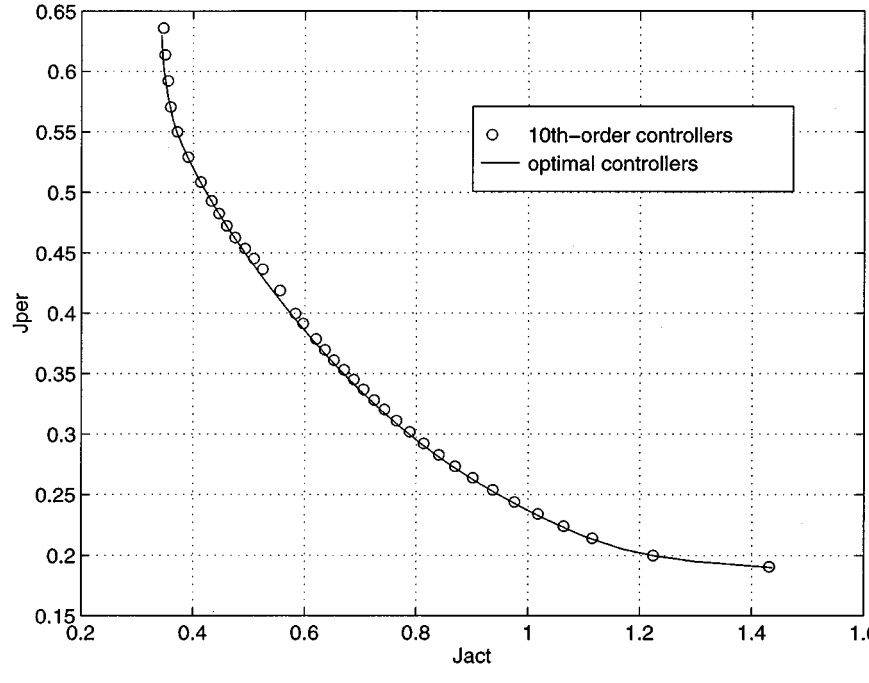

Figure 3. Tradeoff between performance and actuation costs-optimal and reduced-order controllers

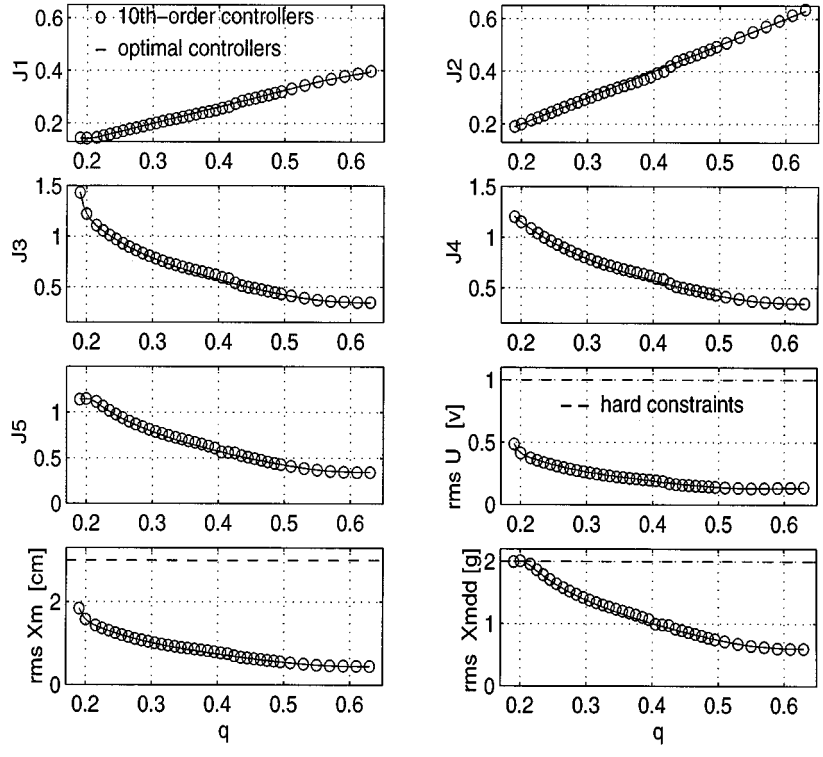

Figure 4. Evaluation criteria—random disturbances—optimal and reduced-order controllers

4.3. *Response to deterministic disturbances*

The time domain specifications, namely costs J_6 to J_{10} and hard constraints in the peak values of u, x_m, and $\ddot{x}_{am}$, for two earthquake records, were not included in the optimization problem (13). Solutions to equation (13) are not guaranteed to satisfy the time domain hard constraints (10), nor the costs J_6 to J_{10} are guaranteed to be optimal in any sense. As a result, further analysis is needed to obtain a set of controllers that meet all specifications.

Figure 5 shows the results of the time-domain analysis for the reduced-order controllers. The subset of reduced-order controllers that meets all constraints is obtained when $q \geqslant 0{\cdot}34$, see frame (4, 2) in Figure 5. Once again, the optimal controllers and the reduced-order controllers show the same behaviour in response to the deterministic disturbances.

4.4. *Admissible controller*

Based on the analysis performed so far, the tenth-order controller with $q = 0{\cdot}34$ gives the best performance for both random and deterministic disturbances. In addition this controller meets all the hard constraints of the problem. A closer examination of the individual SISO transfer functions of this tenth-order controller showed near zero-pole cancelations in each transfer function which were not removed by the model reduction scheme. After removing these near zero-pole cancelations we obtained an eighth-order controller with almost identical performance. We shall refer to this eighth-order controller as the *admissible controller*.

The next three subsections contain the results of several robustness tests that demonstrate that the admissible controller is a good candidate for implementation.

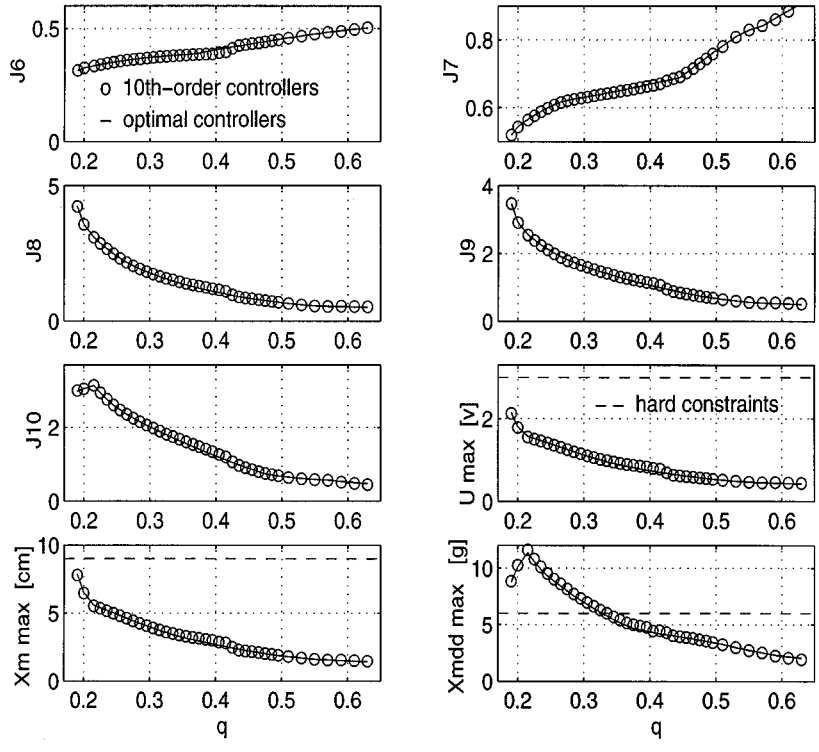

Figure 5. Evaluation criteria—Hachinohe and El Centro earthquakes—optimal and reduced-order controllers

4.5. *Uncertainty in the random disturbance model*

Figures 6 and 7 show, respectively, the values of J_{act} and J_{per} for the eighth-order admissible controller, as the parameters ω_g and ζ_g of the disturbance model (5) vary in the ranges given in equation (8). The plots clearly show that the worst-case closed-loop costs are achieved at the open-loop worst-case values $\omega_{g0} = 5{\cdot}94$ Hz, $\zeta_{g0} = 0{\cdot}3$.

The fact that the worst-case closed-loop parameters ω_g and ζ_g are the worst-case parameters for the uncontrolled structure is not exclusive to $q = 0{\cdot}34$. Variations in the stochastic evaluation criteria with ω_g and ζ_g are shown in Figure 8 for the tenth-order controllers with $q = 0{\cdot}34, 0{\cdot}44, 0{\cdot}54, 0{\cdot}63$. From Figure 8 it follows that all stochastic evaluation criteria reach their maximum value at the open-loop worst-case parameters.

4.6. *Feedback properties and robustness to unmodelled dynamics*

This section contains several frequency-domain tests corresponding to the eighth-order admissible controller. We make use of the following notation. The open-loop transfer matrix from u to y_1 in equations (1) and (2), is denoted by $P_{y_1 u}(s)$. The transfer matrix of the feedback controller C_1 in equation (3) is denoted by $K_1(s)$.

Figure 9 shows the loop gain, with the loop broken at the plant input u; i.e. the magnitude of the frequency response $K_1(j\omega)P_{y_1 u}(j\omega)$. The loop gain is less than $0{\cdot}1$ (-20 db) outside the frequency interval $[5, 31]$ Hz. The roll-offs at high and low frequencies are adequate for the evaluation model is accurate up to 100 Hz.[1] Figure 10 shows the Nyquist plot of $-K_1(j\omega)P_{y_1 u}(j\omega)$. The gain margin is $5{\cdot}4$ at $20{\cdot}9$ Hz. The phase margin is $57{\cdot}1^\circ$ at $18{\cdot}1$ Hz. These are good margins.

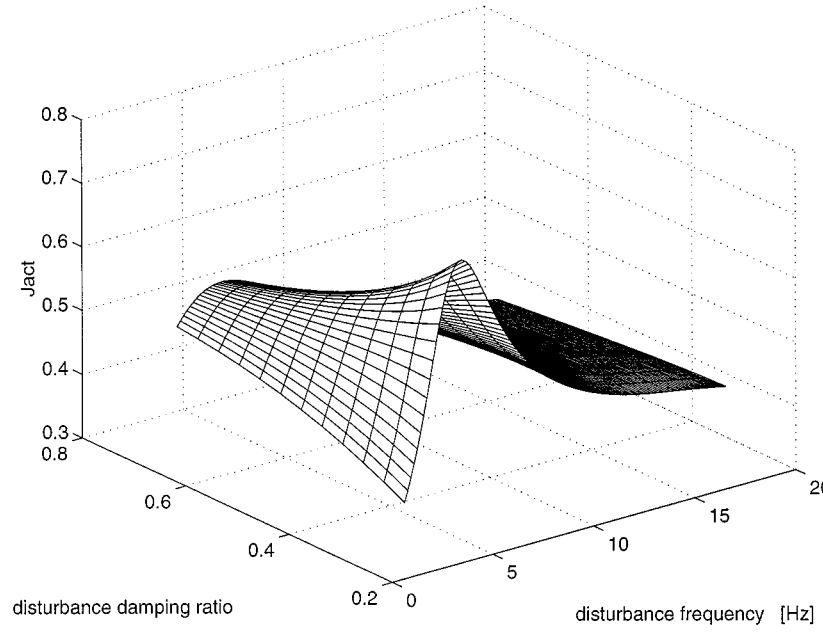

Figure 6. Variation in actuation cost with ω_g and ζ_g for the eighth-order admissible controller

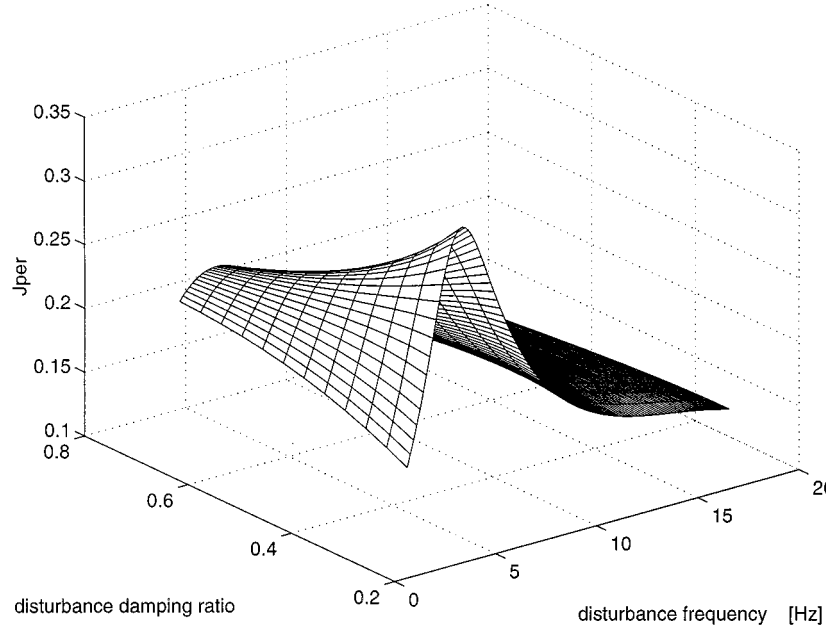

Figure 7. Variation of performance cost with ω_g and ζ_g for the eighth-order admissible controller

Figure 11 shows the variation of the closed-loop poles with the controller gain; i.e. the zeros of the characteristic equation

$$1 - \text{gain } K_1(s)P_{y_1 u}(s) = 0 \tag{14}$$

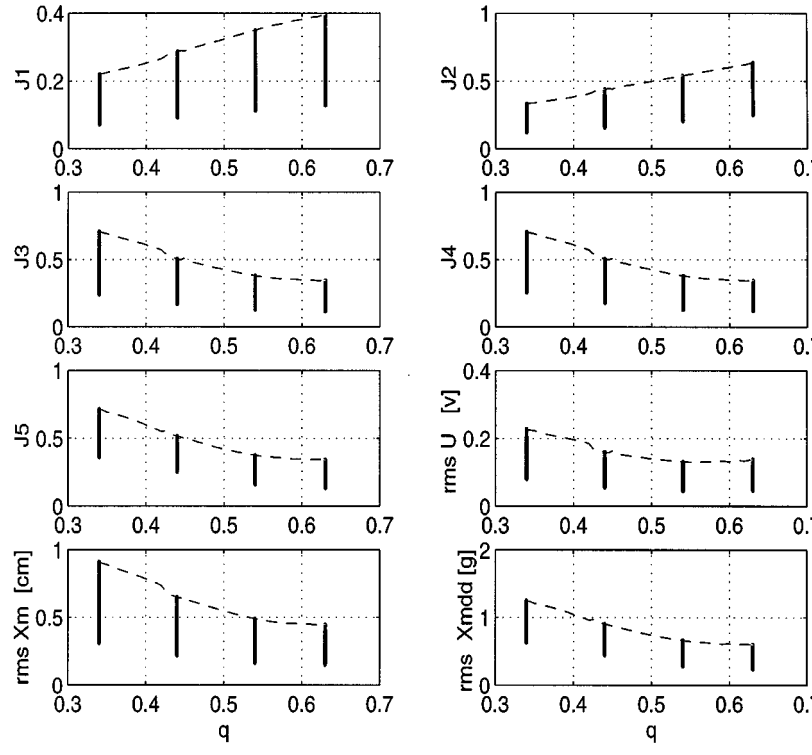

Figure 8. Reduced-order controllers: (●) variation of evaluation criteria with ω_g and ζ_g, (dashed) evaluation criteria with normial ω_g and ζ_g

when the gain is changed from 0 to 5·4 (the gain margin of the system). The three poles close to the imaginary axis are structural modes, the remaining 4 poles are all the controller modes.

From Figures 9 and 11, it follows that the feedback component of the controller improves the structural response by increasing the damping of the first three structural modes without changing their (damped) natural frequencies.

Figure 12 shows the largest singular value ($\sigma_{\max}$) of the complementary sensitivities at plant input and output. These transfer functions are given by

$$T_i(s) = (1 - K_1(s)P_{y_1u}(s))^{-1}K_1(s)P_{y_1u}(s) \quad \text{(at plant input)} \tag{15}$$

$$T_o(s) = (I - P_{y_1u}(s)K_1(s))^{-1}P_{y_1u}(s)K_1(s) \quad \text{(at plant output)} \tag{16}$$

From the plot of $\sigma_{\max}(T_i(j\omega))$ we conclude that noise in the control input u is attenuated at all frequencies. From the plot of $\sigma_{\max}(T_o(j\omega))$ we conclude that noise in the feedback sensors, the linear variable differential transformer and the accelerometers measuring actuator and floor accelerations, is attenuated at all frequencies except for a tiny interval around 18 Hz.

The complementary sensitivities shown in Figure 12 also give the stability margin to multiplicative (or relative) uncertainty at plant input and plant output.[2,3] For example, suppose the true transfer matrix of the structure, from the control input to the feedback sensors, is given by

$$P_{y_1u,\text{true}}(s) = P_{y_1u}(s)(1 + e_i(s)) \tag{17}$$

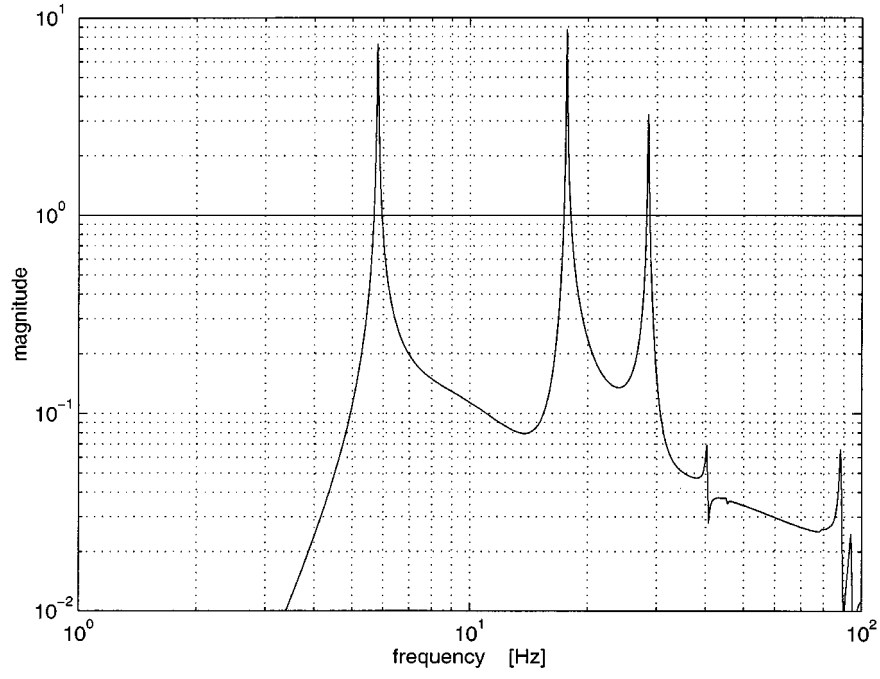

Figure 9. Loop gain with eighth-order admissible controller

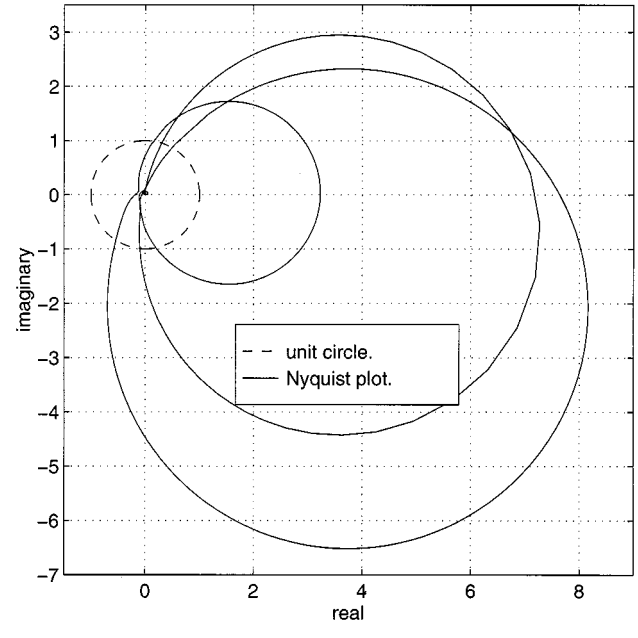

Figure 10. Nyquist plot with eighth-order admissible controller

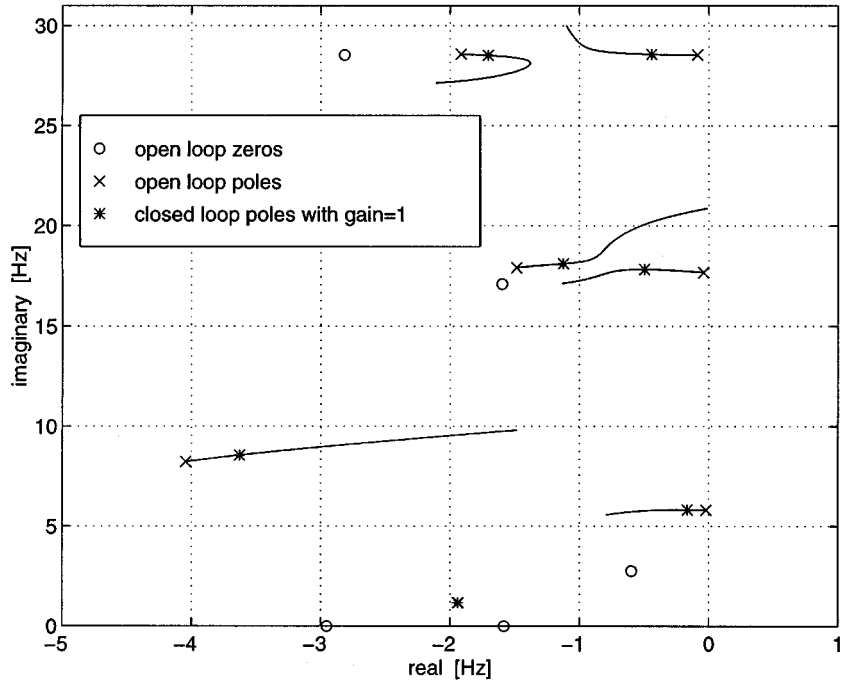

Figure 11. Root locus with eighth-order admissible controller

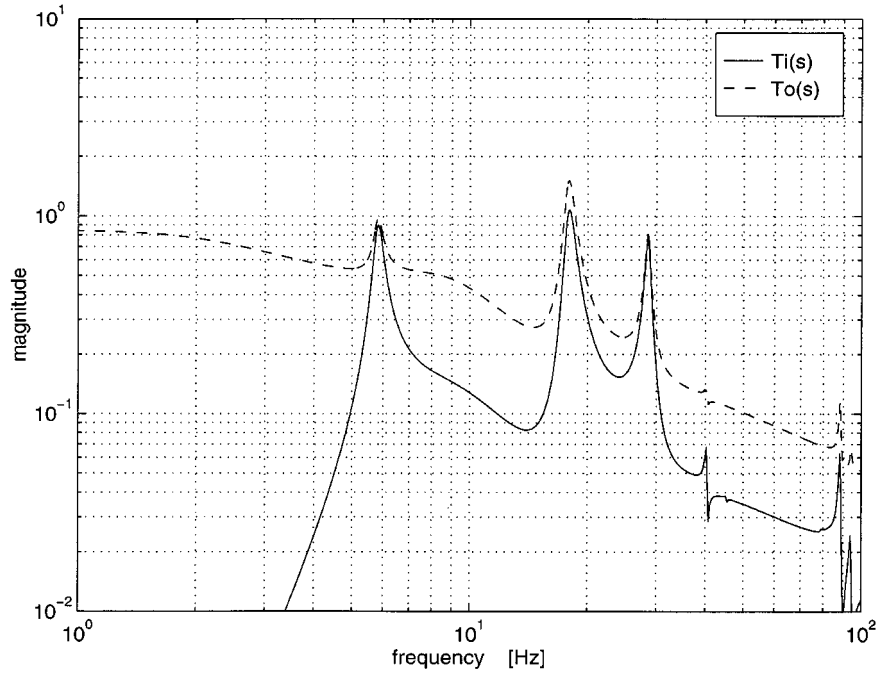

Figure 12. Complementary sensitivities with eight-order admissible controller

where $e_i(s)$ denotes relative modelling error at plant input; e.g., due to unmodeled actuator dynamics. If $e_i(s)$ is stable then the closed-loop system will remain stable as long as

$$|e_i(j\omega)| < \frac{1}{\sigma_{max}(T_i(j\omega))} \tag{18}$$

for all frequencies. Hence, from Figure 12 it follows that e_i could be as large as 100 per cent without de-stabilizing the closed loop; in fact, at frequencies other than the first three structural modes the stability margin is well above 100 per cent. Similarly, the plot of $\sigma_{max}(T_o(j\omega))$ shows that multiplicative perturbations at plant output; i.e., perturbations of the form

$$P_{y_1 u, true}(s) = (I = E_o(s))P_{y_1 u}(s), \tag{19}$$

which account for unmodelled sensor dynamics, could be as large as 100 per cent without destabilizing the closed loop, except for a tiny interval around 18 Hz in which $\sigma_{max}(E_o(j\omega))$ should not exceed 66 per cent.

4.7. *Parametric uncertainty*

A μ test[2,4] was performed to determine stability when the natural frequencies and damping ratios of the first three natural modes are perturbed simultaneously. Recall from the previous subsection that these modes determine the performance of the controlled structure. The nominal frequencies, and damping ratios, of these modes are: $\omega_1 = 5{\cdot}81$ Hz $\zeta_1 = 0{\cdot}33$ per cent, $\omega_2 = 17{\cdot}68$ Hz $\zeta_2 = 0{\cdot}23$ per cent, $\omega_3 = 28{\cdot}53$ Hz $\zeta_3 = 0{\cdot}30$ per cent.

The closed-loop system is guaranteed to remain stable when the structural parameters are perturbed by the following amounts: 21 per cent in natural frequencies (pole magnitude) and 53 per cent in the damping ratios. The upper bound for μ for this simultaneous parameters variation is shown in Figure 13. The interconnection structure required to perform this analysis is given in Appendix III.

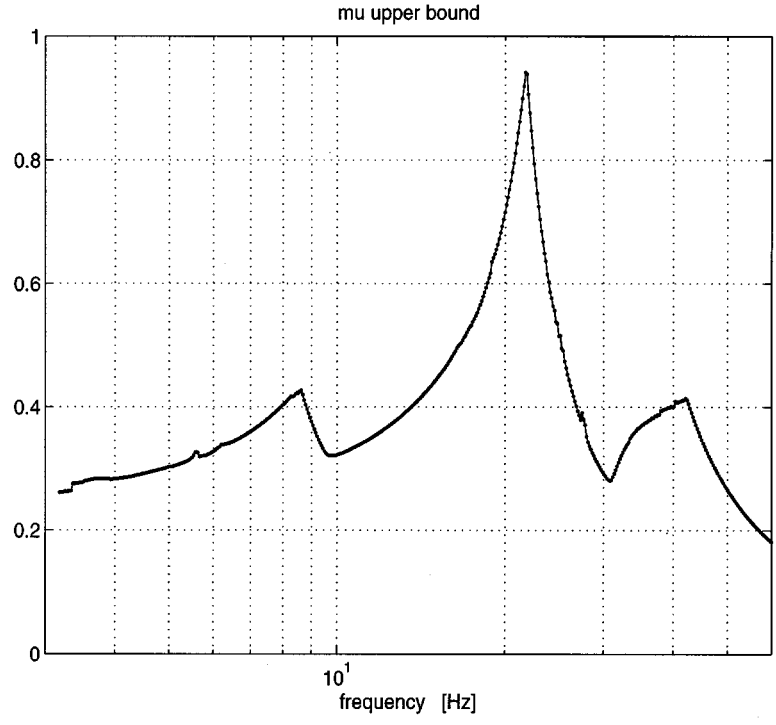

Figure 13. μ upper bound with eighth-order admissible controller

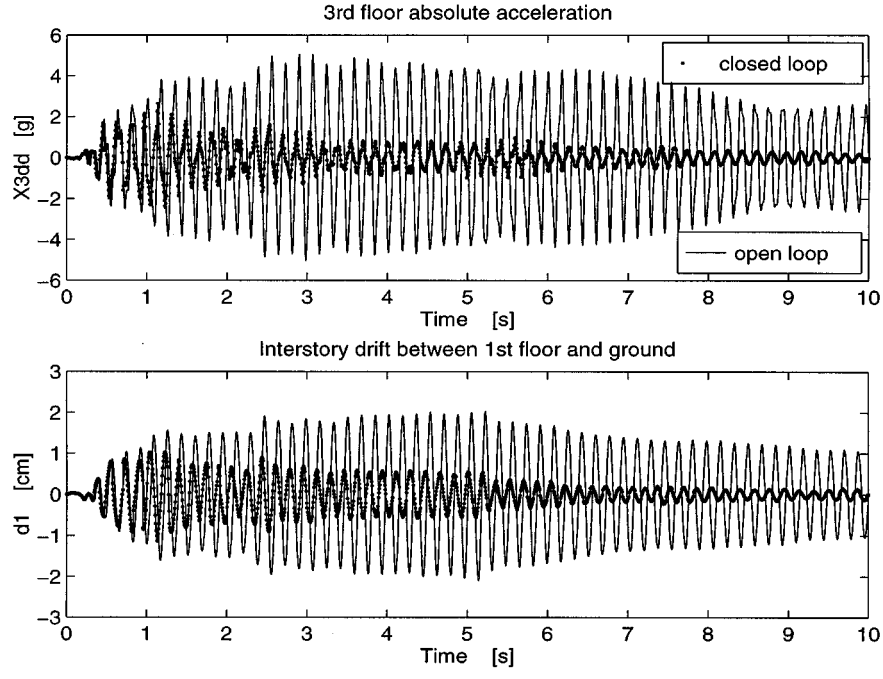

Figure 14. El Centro earthquake disturbance—time histories for 3rd floor acceleration $\ddot{x}_{a3}$ and interstory drift d_1 between 1st floor and ground

5. CONTROLLER VALIDATION

The eighth-order admissible controller was discretized using the bilinear Tustin transform with a 1 kHz sampling rate. Since the magnitudes of the controller zeros and poles are below 31 Hz, the discretization showed no problems with good match between the discrete and continuous time frequency responses. The continuous-time controller is open loop stable (see the controller poles in Figure 11); thus, since we use the bilinear transform, so is the discretized version.

The final linear discrete-time controller was simulated in the time-domain using the non-linear SIMULINK program given in Reference 1. This program contains the linear evaluation model, the A/D and D/A converters with 12-bit precision and a span of ± 3 V, the random and deterministic ground disturbances, and the sensor noises with 0·01 V rms value.

The effectiveness of the controller can be seen by comparing the open- and closed-loop time histories. Figure 14 shows the time histories for the 3rd floor acceleration $\ddot{x}_{a3}$ and the 1st floor interstorey drift d_1, when the system is excited with El Centro earthquake record. Figure 15 shows how these variables respond to the Hachinohe earthquake. We only show the 3rd floor acceleration, and the 1st interstorey drift, because these are the largest acceleration and drift.

From the simulations, we obtained the *actual values* of the evaluation criteria defined in Section 3, with the eighth-order admissible controller. The *analytical values* of the evaluation criteria correspond to the (linear) continuous-time closed loop. The results for the case of random disturbances, are shown in Table II,‡ and the results for the case of deterministic disturbances are shown in Table III.

‡ The *actual values* of the stochastic evaluation criteria were computed using the worst-case parameters ω_g and ζ_g in equation (5) for the linear, continuous-time closed loop, obtained as shown in Section 4.5. The reason for using these worst-case parameters is that the computation of the worst case parameters for the linear system is much less expensive than the computation of those for the non-linear system. This choice is justified in that the non-linear effects considered in the simulations are mild, and then no sensible differences are expected between the worst-case parameters for both systems.

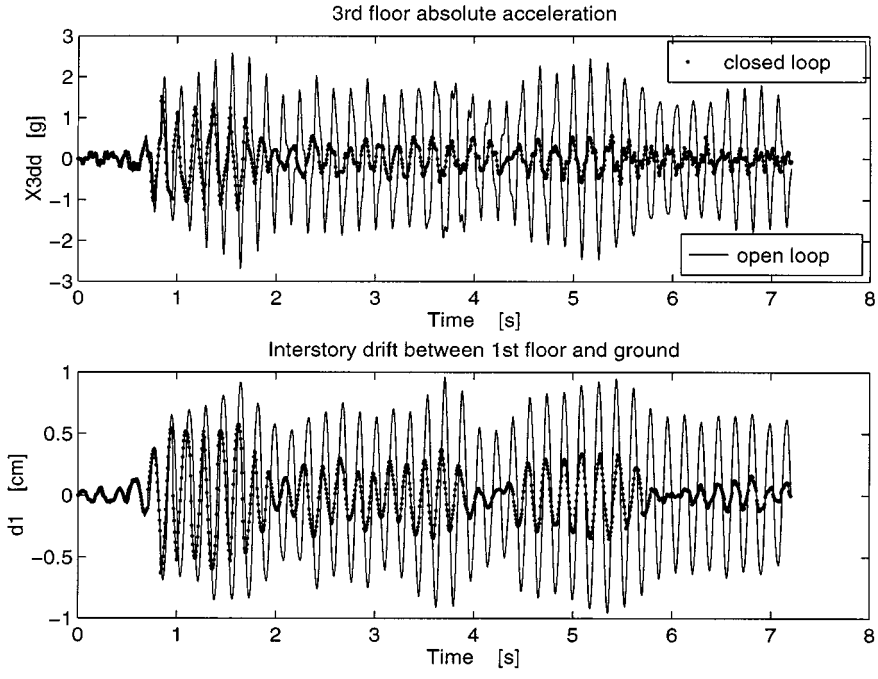

Figure 15. Hachinohe earthquake disturbance—time histories for 3rd floor acceleration $\ddot{x}_{a3}$ and inter-storey drift d_1 between 1st floor and ground

Table II. Evaluation criteria with eighth-order admissible controller—random disturbances. The entries in this table were computed using the value of the scaling factor S_0 in equation (5), and the values of the constants x_{30}, $\dot{x}_{30}$ and $\ddot{x}_{30}$ in equation (6), presented in Reference 1

	Open loop	Closed loop		Reduction (%)
		Analytical	Actual	
J_1	0·5761	0·2139	0·2132	63
J_2	0·9756	0·3207	0·3214	67
J_3	0·0706	0·7028	0·7119	− 908
J_4	0·0706	0·7007	0·7087	− 904
J_5	1·0429	0·7090	0·6859	34
σ_u	0	0·2340 V	0·2278 V	N/A
σ_{x_m}	0·0925 cm	0·9417 cm	0·9326 cm	− 908
$\sigma_{\ddot{x}_{am}}$	1·8667g	1·2993g	1·2278g	34

The following conclusion is immediate from these tables: *The controller reduces the random interstorey drift, and floor acceleration, responses by 63 per cent, or more. The controller reduces the deterministic interstorey drift, and floor acceleration, responses by 39 per cent. All hard constraints are met.*

Table III. Evaluation criteria with eighth-order admissible controller—Hachinohe and El Centro earthquakes

	Open loop	Closed loop		Reduction (%)
		Analttical	Actual	
J_6	0·6201	0·3800	0·3797	39
J_7	1·043	0·6431	0·6398	39
J_8	0·07721	1·484	1·4778	− 1814
J_9	0·083	1·395	1·3909	− 1576
J_{10}	1·139	1·712	1·6827	− 48
$\|u\|_{\max}$	0	0·9748 V	0·9771 V	N/A
$\|x_{\mathrm{m}}\|_{\max}$	0·2458 cm	3·458 cm	3·4616 cm	− 1308
$\|\ddot{x}_{\mathrm{am}}\|_{\max}$	5·428cm	5·858g	5·8105g	− 7

APPENDIX I

Solution to optimization problem

The optimization problem (13) is solved using the method presented in Reference 5.

Step 1: Obtain a realization for the linear time invariant system that includes the structural model equation (1), the stochastic ground disturbance model equation (5), and the white measurement noise, of the form

$$\dot{\eta} = A\eta + B_1 \begin{bmatrix} w_{\mathrm{g}} \\ v_n \end{bmatrix} + B_2 u \tag{20a}$$

$$z = C_1\eta + D_{11} \begin{bmatrix} w_{\mathrm{g}} \\ v_n \end{bmatrix} + D_{12} u \tag{20b}$$

$$y = C_2\eta + D_{21} \begin{bmatrix} w_{\mathrm{g}} \\ v_n \end{bmatrix} + D_{22} u \tag{20c}$$

The signal w_{g} is a normalized (unit spectral density) white noise process representing the input to the disturbance model, v_n is the normalized sensor noise process uncorrelated with w_{g}, u is the control signal (in volts), and y is the six-component measurement vector (in volts). The vector of controlled responses z has twelve components and it is defined by

$$z_1 = r_3 \frac{x_{\mathrm{m}}}{\sigma_{x_{3\mathrm{o}}}} \qquad z_7 = \frac{r_1 d_1}{q J_{\mathrm{per}}^{\mathrm{OL}} \sigma_{x_{3\mathrm{o}}}}$$

$$z_2 = r_4 \frac{\dot{x}_{\mathrm{m}}}{\sigma_{\dot{x}_{3\mathrm{o}}}} \qquad z_8 = \frac{r_1 d_2}{q J_{\mathrm{per}}^{\mathrm{OL}} \sigma_{x_{3\mathrm{o}}}}$$

$$z_3 = \frac{\ddot{x}_{\mathrm{am}}}{\sigma_{\ddot{x}_{\mathrm{a}3\mathrm{o}}}} \qquad z_9 = \frac{r_1 d_3}{q J_{\mathrm{per}}^{\mathrm{OL}} \sigma_{x_{3\mathrm{o}}}}$$

$$z_4 = \frac{u}{1\ \mathrm{V}} \qquad z_{10} = \frac{\ddot{x}_1}{q J_{\mathrm{per}}^{\mathrm{OL}} \sigma_{\ddot{x}_{\mathrm{a}3\mathrm{o}}}}$$

$$z_5 = \frac{\ddot{x}_{\mathrm{am}}}{2\,g} \qquad z_{11} = \frac{\ddot{x}_2}{qJ^{\mathrm{OL}}_{\mathrm{per}}\sigma_{\ddot{x}_{\mathrm{a}30}}}$$

$$z_6 = \frac{x_{\mathrm{m}}}{3\ \mathrm{cm}} \qquad z_{12} = \frac{\ddot{x}_3}{qJ^{\mathrm{OL}}_{\mathrm{per}}\sigma_{\ddot{x}_{\mathrm{a}30}}}$$

where q and $J^{\mathrm{OL}}_{\mathrm{per}}$ are as in equation (13).

Define the exogenous input $w = [w_{\mathrm{g}}^{\mathrm{T}} v_n^{\mathrm{T}}]^{\mathrm{T}}$. Pick a stabilizing controller C (see equation (4)) and let $T_{z_i w}$ denote the closed-loop transfer matrix from w to z_i, for $i = 1, \ldots, 12$. Standard results[6] show that the optimization problem (13) is equivalent to the following problem:

$$\min_{C} \gamma \text{ subject to} \tag{21a}$$

$$\| T_{z_i w} \|_2 < \gamma \quad i = 1, \ldots, 3$$

$$\| T_{z_i w} \|_2 < 1 \quad i = 4, \ldots, 12$$

where the minimization is performed over all stabilizing controllers C and the symbol $\| \cdot \|_2$ denotes the $\mathscr{H}_2$ norm of a transfer matrix defined by

$$\| T \|_2 = \sqrt{\frac{1}{2\pi} \operatorname{trace} \int_{-\infty}^{\infty} T(\mathrm{j}\omega) T^*(\mathrm{j}\omega)\, \mathrm{d}\omega}$$

The formulas presented in the following steps are valid for $D_{11} = 0$, a condition that holds for equation (20).

Step 2: Obtain the real, symmetric, stabilizing solution $\bar{Y}$ to the algebraic Riccati equation

$$AY + YA^{\mathrm{T}} + B_1 B_1^{\mathrm{T}} - (TC_2^{\mathrm{T}} + B_1 D_{21}^{\mathrm{T}})(D_{21} D_{21}^{\mathrm{T}})^{-1}(C_2 Y + D_{21} B_1^{\mathrm{T}}) = 0.$$

Step 3: Given $\bar{Y}$ and a small number β,[5] and any real symmetric Q_{p} and any real W_{p} satisfying the linear equation

$$AQ_{\mathrm{p}} + Q_{\mathrm{p}} A^{\mathrm{T}} + B_2 W_{\mathrm{p}} + W_{\mathrm{p}}^{\mathrm{T}} B_2^{\mathrm{T}} + (\bar{Y} C_2^{\mathrm{T}} + B_1 D_{21}^{\mathrm{T}})(D_{21} D_{21}^{\mathrm{T}})^{-1}(C_2 \bar{Y} + D_{21} B_1^{\mathrm{T}}) + \beta 1 = 0$$

which has solution because (A, B_2) is stabilizable.

Step 4: Find a basis $\{(Q_j, W_j)\}_{j=1, \ldots, r}$ for the linear subspace

$$\{(Q, W) : Q = Q^{\mathrm{T}},\ AQ + QA^{\mathrm{T}} + B_2 W + W^{\mathrm{T}} B_2^{\mathrm{T}} = 0\}$$

Step 5: Solve the following convex optimization problem on the scalar variables $\gamma^2, a_1, \ldots, a_r$:

$$\min \gamma^2 \text{ subject to} \tag{22}$$

$$\begin{bmatrix} \gamma^2 - C_{1i} \bar{Y} C_{1i}^{\mathrm{T}} & C_{1i} Q + D_{1i} W \\ (C_{1i} Q + D_{1i} W)^{\mathrm{T}} & Q \end{bmatrix} \geqslant 0, \quad i = 1, \ldots, 3$$

$$\begin{bmatrix} 1 - C_{1i} \bar{Y} C_{1i}^{\mathrm{T}} & C_{1i} Q + D_{1i} W \\ (C_{1i} Q + D_{1i} W)^{\mathrm{T}} & Q \end{bmatrix} \geqslant 0 \quad i = 4, \ldots, 12$$

$$Q = Q_p + \sum_{j=1}^{r} a_j Q_j$$

$$W = W_p + \sum_{j=1}^{r} a_j W_j$$

where $C_{1i}(D_{1i})$ is the ith row of $C_1(D_1)$. Problem (22) can be efficiently solved using standard software tools.[7]

Step 6: Denote an optimal solution to equation (22) by $\{\gamma^{\mathrm{OPT}}, a_1^{\mathrm{OPT}}, \ldots, a_r^{\mathrm{OPT}}\}$, and define the optimal matrices Q^{OPT} and W^{OPT} as follows:

$$Q^{\mathrm{OPT}} = \sum_{j=1}^{r} a_j^{\mathrm{OPT}} Q_j$$

$$W^{\mathrm{OPT}} = \sum_{j=1}^{r} a_j^{\mathrm{OPT}} W_j$$

A stabilizing controller solving equation (13) has the following realization:

$$\left[\begin{array}{c|c} A_k & B_k \\ \hline C_k & D_k \end{array}\right] = \left[\begin{array}{c|c} A + HC_2 + B_2F + HD_{22}F & -H \\ \hline F & 0 \end{array}\right]$$

where $F = W^{\mathrm{OPT}}(Q^{\mathrm{OPT}})^{-1}$ and $H = -(\bar{Y}C_2^{\mathrm{T}} + B_1D_{21}^{\mathrm{T}})(D_{21}D_{21}^{\mathrm{T}})^{-1}$.

APPENDIX II

Controller reduction

This appendix describes the procedure used to obtain reduced-order controllers. The reduction was performed applying the weighted balance and truncation method on a controller coprime factorization, where the weight is chosen to preserve closed loop stability. The method is presented in References 8 and 2. The two procedures described below correspond to the truncation of left and right controller factorizations.

Stability weighted left coprime factorization

Step 1: Find a left coprime factorization $(\tilde{V}(s), \tilde{U}(s))$[2, 3] of the controller transfer matrix $K(s)$; e.g., compute stable matrices $(\tilde{V}(s), \tilde{U}(s))$ satisfying $K(s) = \tilde{V}^{-1}(s)\tilde{U}(s)$.

Step 2: Obtain a minimal realization for the weight $W(s)$ defined by

$$W(s) = \begin{bmatrix} -P_{yu}(s) \\ I \end{bmatrix} (I - K(s)P_{yu}(s))^{-1}\tilde{V}^{-1}(s)$$

where $P_{yu}(s)$ is the transfer matrix from control signal u to the measurement vector y, which is stabilized by the controller $K(s)$.

Step 3: Apply the weighted balance and truncation method, given in References 8, 2 and 9, to the system

$$[\tilde{U}(s) \quad \tilde{V}(s)]W(s)$$

to obtain the reduced-order coprime factors

$$[\hat{\tilde{U}}(s) \quad \hat{\tilde{V}}(s)]$$

The reduced-order controller $\hat{K}(s)$ is given by

$$\hat{K}(s) = \hat{\tilde{V}}^{-1}(s)\hat{\tilde{U}}(s)$$

and it is guaranteed to stabilize the system $P_{yu}(s)$ if

$$\| [\tilde{U}(s) - \hat{\tilde{U}}(s) \quad \tilde{V}(s) - \hat{\tilde{V}}(s)]W(s) \|_\infty < 1$$

Stability weighted right coprime factorization

Step 1: Find a right coprime factorization $(V(s), U(s))$ of the controller transfer matrix $K(s)$; e.g. compute stable matrices $(V(s), U(s))$ satisfying $K(s) = U(s)V^{-1}(s)$.

Step 2: Obtain a minimal realization for the weight $W(s)$ defined by

$$W(s) = V^{-1}(s)(I - P_{yu}(s)K(s))^{-1}[-P_{yu}(s) \quad I]$$

where P_{yu} is the transfer matrix from control signal u to measurement vector y, which is stabilized by the controller $K(s)$.

Step 3: Apply the weighted balance and truncation method, given in References 8, 2 and 9, to the system

$$W(s)\begin{bmatrix} U(s) \\ V(s) \end{bmatrix}$$

to obtain the reduced-order coprime factors

$$\begin{bmatrix} \hat{U}(s) \\ \hat{V}(s) \end{bmatrix}$$

The reduced-order controller $\hat{K}(s)$ is given by

$$\hat{K}(s) = \hat{U}(s)\hat{V}^{-1}(s)$$

and is guaranteed to stabilize the system $P_{yu}(s)$ if

$$\left\| W(s)\begin{bmatrix} U(s) - \hat{U}(s) \\ V(s) - \hat{V}(s) \end{bmatrix} \right\|_\infty < 1$$

APPENDIX III

Interconnection structure for μ test

The μ-set in Section 4.7 requires a description of the parametric uncertainty, in the first three structural modes, for the transfer matrix $P_{y_1 u}$ from u to y_1 defined in equations (1) and (2).

Step 1: Use the evaluation model to compute the following expansion for the nominal $P_{y_1 u}$:

$$P_{y_1 u}(s) = \sum_{i=1}^{3} \frac{C_{i1}s + C_{i2}}{s^2 + 2\zeta_{i0}\omega_{i0}s + \omega_{i0}^2} + R(s) \tag{23}$$

where the first three terms contain the dynamics of the first three structural modes, and R contains the remaining dynamics. In equation (23), C_{ij} is a column vector of dimension five, ω_{i0} and ζ_{i0} are the nominal frequency and damping ratio of mode i.

Step 2: Model the perturbations in the natural frequencies and damping ratios, of the first three structural modes, using the equations

$$P_{y_1 u}^{\text{per}} = \sum_{i=1}^{3} P^i(s) + R(s) \tag{24a}$$

$$P^i(s) = \frac{C_{i1}s + C_{i2}(\omega_i/\omega_{i0})^2}{s^2 + 2\zeta_i\omega_i s + \omega_i^2} \tag{24b}$$

where $\omega_i = \omega_{i0}(1 + W_{\omega_i}\delta_{\omega_i})$, $\zeta_i = \zeta_{i0}(1 + W_{\zeta_i}\delta_{\zeta_i})$, δ_{ω_i} and δ_{ζ_i} denote real parametric variations with magnitude less than one, $W_{\omega_i} > 0$ and $W_{\zeta_i} > 0$ specify the size of the uncertainty and are defined by the user. Notice, from equation (24b), that the high and low-frequency behaviour of $P^i(s)$ is independent of the perturbations in ω_i and ζ_i.

Step 3: Isolate the uncertain parameters in equation (24b) by writing each uncertain component $P^i(s)$ as follows:

$$P^i(s) = G^i_{22}(s) + G^i_{21}(s)\Delta^i(I - G^i_{11}\Delta^i)^{-1}G^i_{12}(s) \tag{25a}$$

$$\begin{bmatrix} G^i_{11} & G^i_{12} \\ G^i_{21} & G^i_{22} \end{bmatrix} = \begin{bmatrix} C^i_1 \\ C^i_2 \end{bmatrix}(sI - A^i)^{-1}[B^i_1 \; B^i_2] + \begin{bmatrix} D^i_{11} & 0 \\ D^i_{21} & 0 \end{bmatrix} \tag{25b}$$

$$\Delta^i = \begin{bmatrix} \delta_{\omega_i} & 0 & 0 \\ 0 & \delta_{\omega_i} & 0 \\ 0 & 0 & \delta_{\zeta_i} \end{bmatrix} \tag{25c}$$

where

$$A^i = \begin{bmatrix} 0 & \omega_{0i} \\ -\omega_{0i} & -2\zeta_{0i}\omega_{0i} \end{bmatrix}, \quad B^i_1 = \begin{bmatrix} W_{\omega_i} & 0 & 0 \\ -2\zeta_{0i}W_{\omega_i} & -W_{\omega_i} & -W_{\zeta_i} \end{bmatrix}, \quad B^i_2 = \begin{bmatrix} 0 \\ 1 \end{bmatrix}$$

$$C^i_1 = \begin{bmatrix} 0 & \omega_{0i} \\ \omega_{0i} & 0 \\ 0 & 2\zeta_{0i}\omega_{0i} \end{bmatrix}, \quad D^i_{11} = \begin{bmatrix} 0 & 0 & 0 \\ 0 & 0 & 0 \\ 2\zeta_{0i}W_{\omega_i} & 0 & 0 \end{bmatrix}$$

$$C^i_2 = \begin{bmatrix} \dfrac{1}{\omega_{0i}}C_{i2} & C_{i1} \end{bmatrix}, \quad D^i_{21} = \begin{bmatrix} 0 & \dfrac{W_{\omega_i}}{\omega^2_{0i}}C_{i2} & 0 \end{bmatrix}$$

It now follows from (24a) and (25a) that the perturbed transfer matrix $P^{\text{per}}_{y_1u}(s)$ is the transfer matrix, from u to y_1, in the block diagram shown in Figure 16, where the transfer matrix G^i is given by

$$G^i = \begin{bmatrix} G^i_{11} & G^i_{12} \\ G^i_{21} & G^i_{22} \end{bmatrix}$$

Thus, $P^{\text{per}}_{y_1u}(s)$ is now in the format necessary for the μ test [4, 2].

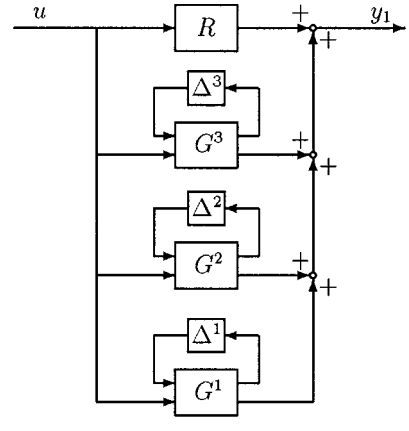

Figure 16. Interconnection structure for μ test

ACKNOWLEDGEMENTS

This work was supported in part by the National Science Foundation under The Young Investigator Award ECS-9358288, and in part by Boeing and United Technologies corporations.

REFERENCES

1. B. F. Spencer Jr., S. J. Dyke and H. S. Deoskar, 'Benchmark problems in structural control. Parts I and II', in *Structures Congress*, ASCE, Portland, Oregon, April 1997.
2. K. Zhou, J. C. Doyle and K. Glover, *Robust and Optimal Control*, Prentice-Hall, Englewood Cliffs, NJ 1996.
3. M. Green and D. Limebeer. *Linear Robust Control*, Prentice-Hall, Englewood Cliffs, NJ, 1995.
4. G. Balas, J. Doyle, K. Glover and R. Smith, *μ-Analysis and Synthesis Toolbox*. The MathWorks, Inc., 1995.
5. M. A. Rotea, 'The generalized $\mathscr{H}_2$ control problem', *Automatica* **29**, 373–386 (1983).
6. H. Kwakernaak and R. Sivan. *Linear Optimal Control Systems*. Wiley-Interscience, New York, 1972.
7. P. Gahinet, A., Nemirovski, A. Laub and M. Chilali, *LMI Control Toolbox*. The MathWorks, Inc., 1995.
8. B. D. O. Anderson and Y. Liu, 'Controller reduction: concepts and approaches', *IEEE Trans. Automat. Control* **34**, 802–812 (1989).
9. D. Enns, 'Model reduction for control system design', *Ph.D. thesis*, Stanford University, Stanford, California, 1984.

